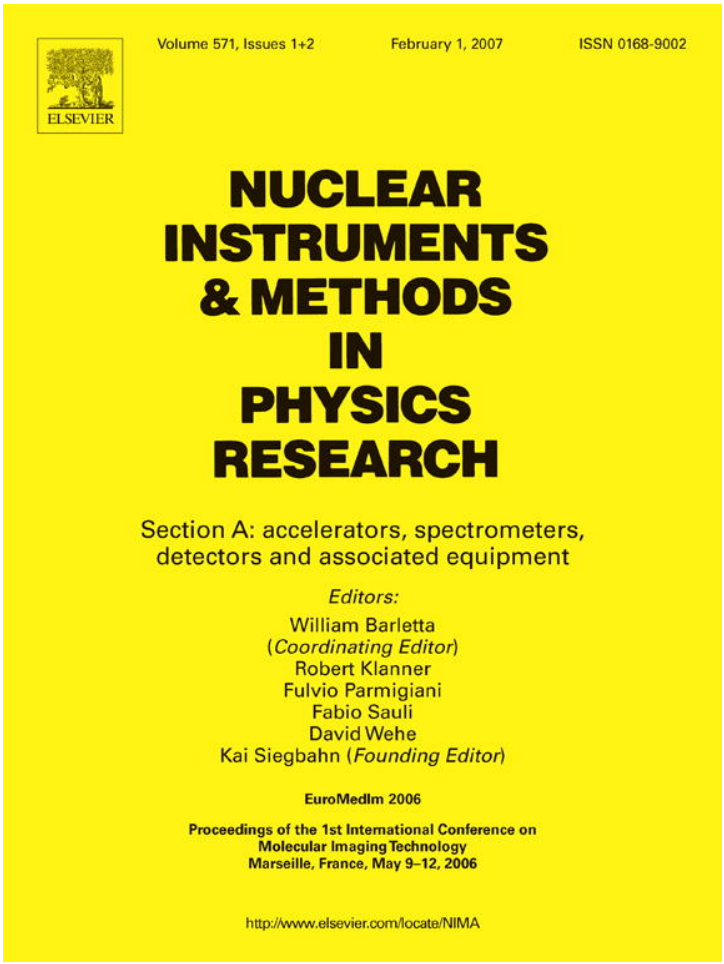

Available online at www.sciencedirect.com
ScienceDirect
Nuclear Instruments and Methods in Physics Research A 571 (2007) 419–424
NUCLEAR INSTRUMENTS & METHODS IN PHYSICS RESEARCH Section A
www.elsevier.com/locate/nima

Scintillator studies for the HPD-PET concept

A. Braem[b], E. Chesi[b], F. Ciocia[a], R. De Leo[a,*], C. Joram[b], L. Lagamba[a], E. Nappi[a], J. Séguinot[b], I. Vilardi[a], P. Weilhammer[b]

[a]*Physics Department and INFN Section of Bari, Via Orabona 4, Bari, Italy*
[b]*CERN PH-Department, CH-1211 Geneva, Switzerland*

Available online 13 November 2006

Abstract

The spatial, energy, and time resolutions of 10 cm long polished YAP:Ce and LYSO:Ce crystals have been measured. The work is part of the novel HPD-PET concept, based on a full three-dimensional, free of parallax errors, reconstruction of the γ-ray interaction point in 10–15 cm long scintillators. The effective light attenuation length, a key parameter of the HPD-PET concept, and the resolutions have been measured for various wrappings and coatings of the crystal lateral surfaces. Even if the final HPD-PET prototype could use scintillators and/or wrappings different from those tested, the results here presented prove the feasibility of the concept and provide hints on its potential capabilities.

PACS: 29.40.Mc; 29.30.Kv; 87.58.Fg

Keywords: YAP:Ce; LYSO:Ce; Molecular imaging; PET; HPD

1. Introduction

Molecular imaging by PET is a powerful tool in modern clinical practice for cancer diagnosis. Nevertheless, new PET concepts are needed for specific applications to some human organs, as breast, prostate, brain, etc.

Presently, commercially available PET scanners do not detect the depth of interaction (DoI) of γ-rays in scintillators, which results in a parallax error. Crystal lengths of few centimetres are commonly used to limit this error.

The CIMA collaboration [1] has proposed a novel 3D PET geometrical concept [2] based on axially oriented arrays of long (10–15 cm) polished scintillator bars read out at the two ends by hybrid photodetectors (HPD) [3]. A schematic view of one module of the novel device is shown in Fig. 1. An unambiguous definition of the DoI is made possible from the read out of charges at both the crystal ends. The final PET will be made by several of these modules, whose spatial distribution will be different depending on the human organ to examine.

The HPD-PET concept is new compared to commercially available PETs which are based [2] on a radial displacement of crystals in the module, on a shorter crystal length, and on a different finishing (raw) of the crystal lateral surface. The 3D Axial HPD-PET concept can provide higher efficiency, due to the absence of limitations imposed by the detector thickness in the radial direction, and to the possibility [4] to recover a fraction of γ's undergoing double interactions (first Compton and then photoelectric) in the same module.

Studies reported in literature on PET designs [5–8] where the DoI information is obtained reading out both the crystal ends [9], refer to shorter scintillator bars (2–3 cm) with their lateral surfaces finished differently (raw) from our concept, favouring more the diffuse reflection of scintillation light on the crystal lateral surfaces, rather than the specular reflection.

In fact, scintillation light propagates to the two ends of a polished crystal by internal reflection on lateral surfaces. On its way to the photodetectors, part of the light is absorbed with a characteristic attenuation length λ_{eff},

*Corresponding author. Tel.: +39 80 54 43 242; fax: +39 80 55 34 938.
E-mail address: deleo@ba.infn.it (R. De Leo).

0168-9002/$ - see front matter © 2006 Elsevier B.V. All rights reserved.
doi:10.1016/j.nima.2006.10.124

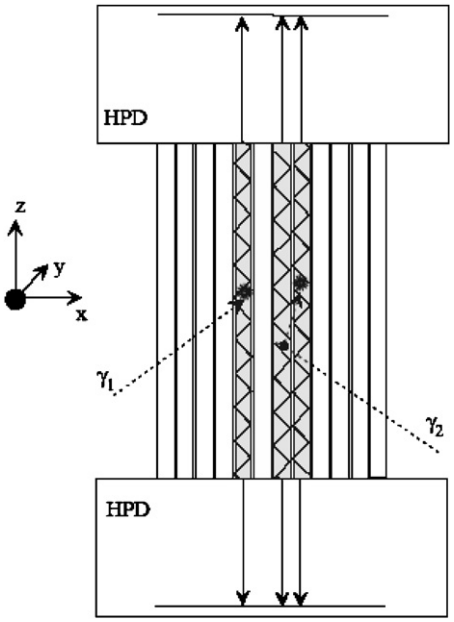

Fig. 1. Schematic illustration of one module of the 3D axial HPD-PET concept. Matrices of axially arranged long crystals are read out on both sides by HPDs.

which is different from the bulk value λ_{bulk} as it takes into account the real path of the photons. While the transverse coordinates (x,y) of the detected γ-ray are determined from the address (i.e. position) of the hit crystal, deduced by both photodetectors with a spatial resolution [2] $\sigma_{x,y} = 3.2\,\text{mm}/\sqrt{12} = 0.92\,\text{mm}$, the axial (z) coordinate is derived with a precision σ_z from the ratio of the photoelectron yield, N_1 and N_2, measured at the two ends of the crystal with length L_C:

$$z = \frac{1}{2}\left(\lambda_{\text{eff}} \ln \frac{N_1}{N_2} + L_C\right)$$

$$\sigma_z(z) = \frac{\lambda_{\text{eff}}}{\sqrt{2N_o}}\left(\exp\frac{z}{\lambda_{\text{eff}}} + \exp\frac{L_C - z}{\lambda_{\text{eff}}}\right)^{1/2}. \quad (1)$$

The expression reported for σ_z accounts only for the photoelectron statistical uncertainty. N_0 is the number of photoelectrons for $\lambda_{\text{eff}} \to \infty$, or, equivalently for $z \to 0$. Its value depends both on the physical and optical properties of the chosen scintillator, including its surface finishing (coating/wrapping) and on the characteristics of the photodetector. It is implicitly assumed that the photoelectron yields N_1 and N_2 depend exponentially on the average path length of the scintillation photons belonging to one gamma:

$$N_1(z) = \frac{N_0}{2}\exp\left(\frac{-z}{\lambda_{\text{eff}}}\right)$$

$$N_2(z) = \frac{N_0}{2}\exp\left(\frac{-(L_C - z)}{\lambda_{\text{eff}}}\right) \quad (2)$$

giving the total number of detected photoelectrons N_{pe}:

$$N_{pe}(z) = N_1(z) + N_2(z). \quad (3)$$

The statistical term of the energy and time resolutions can be expressed as:

$$\frac{\sigma_E}{E}(z) = \sqrt{\frac{\text{ENF}}{N_{pe}(z)}} \oplus R_{\text{int}}$$

$$\sigma_T = \frac{c}{\sqrt{N_{pe}(z)}} \quad (4)$$

where ENF is the excess noise factor [10] of the photodetector, c is a constant, and R_{int} is the scintillator intrinsic resolution.

From the previous equations it can be seen that while an increase of N_0 improves all the resolutions, an increase of λ_{eff}, although improving σ_E/E and σ_T, worsens σ_z. In order to achieve a competitive σ_z value, the crystal length L_C needs to be limited to values below $\sim$150 mm and λ_{eff} has to be optimized depending on the chosen crystal and its length. Thus the three parameters N_0, L_C, and λ_{eff}, corresponding, respectively, to scintillator type, length, and wrapping/coating, play a key role in the proposed geometrical PET concept.

In this paper we present an experimental study to optimize the effective light attenuation length, λ_{eff}, for a set of polished YAP:Ce scintillators of dimensions $3.2 \times 3.2 \times 100\,\text{mm}^3$ produced by Preciosa Crytur Co at Turnov, Czech Republic, and for a few samples of polished LYSO:Ce of equal size, produced by Photonic Materials, Bellshill, Scotland. We have measured the λ_{eff} parameter in polished and wrapped/coated crystals by means of 511 keV γ-rays emitted from a ^{22}Na source. The Litrani photon tracking code [11] will be used to predict results for other crystal lengths and scintillators that will be presumably employed in the final device.

2. Experimental setup and results

We have carried out the experimental studies with YAP and LYSO crystals of dimensions $3.2 \times 3.2 \times 100\,\text{mm}^3$. Their refractive indices (at the emission wavelength maximum) are $n_{\text{LYSO}} = 1.82$ (420 nm), and $n_{\text{YAP}} = 1.94$ for YAP (370 nm). The thickness of the crystal has been chosen to match the segmentation of the HPDs that will be used in the final project [2,3]. These will be equipped with a thin sapphire window ($n = 1.793$ at 370 nm, $n = 1.782$ at 420 nm), thus leading to an almost perfect refractive index matching which minimizes transmission losses at the crystal–detector interface.

For the present study two H3164-10 PMTs† with bialkali photocathodes and borosilicate windows ($n_{\text{win}} = 1.47$) have been used as photodetectors. The PMTs are coupled to the scintillator with optical grease (BC-630 from Bicron, $n_{\text{BC-630}} = 1.47$). The HPDs of the final device will be equipped with a thin sapphire window ($n = 1.793$ at 370 nm, $n = 1.782$ at 420 nm), thus leading to an almost perfect refractive index matching which minimizes transmission losses at the crystal-detector interface. In this latter case, a thin layer of an optical coupling oil, one of those

commercialized by Cargille-Sacher Laboratories Inc. [12], with refractive indices higher than that of BC-630, will be used.

The crystal-PMTs complex is placed on a linear stage remotely movable by a step motor in order to produce scintillations at different DoIs in the crystal. A point-like ^{22}Na source sealed in plastic has been used. One of the two resulting 511 keV γ-rays is detected by the crystal that is placed in coincidence with a cylindrical BaF_2 scintillator detecting the second 511 keV γ-ray. The BaF_2 detector and the γ-source are placed at a fixed position outside of the linear stage. The radioactive source is collimated with a 4 mm lead shield block with a rectangular opening in order to illuminate a 2 mm wide slide of the crystal lateral surface.

Conventional NIM electronics has been used. The data acquisition has been restricted to coincident timing signals from the crystal-left, crystal-right and BaF_2 PMTs. Timing signals have been formed by employing constant fraction discriminators (CFD).

An example of the obtained spectra (sum of the left and right signals) for polished YAP and LYSO crystals with 511 keV γ-rays impinging at the crystal centre ($z = 5$ cm) is shown in Fig. 2. The LYSO scintillator has a higher photofraction and produces more photoelectrons than YAP, as a consequence of a higher photon yield [2] (23 ph/keV for LYSO, 18 ph/keV for YAP), of a lower refractive index, and, as will be shown later, of a longer light attenuation length. But, in spite of the higher photoelectron number, the energy resolution of LYSO is worse than that of YAP, most probably due to a higher intrinsic resolution [2,13]. The $\Delta E/E$ (FWHM) values are: 10.8% for YAP and 14.6% for LYSO. This last value is comparable with those quoted in literature: 13–15% of Ref. [6] and 14–18% of Ref. [5], both obtained for 20 mm long LSO raw bars. The YAP energy resolution is better than the 14% value quoted in Ref. [13] for 30 mm long bars.

To measure the energy linearity of the two scintillators, an important parameter in our project to recover a fraction of γ's undergoing double interactions (first Compton and then photoelectric) in a crystal module, a similar setup has been used employing various radioactive sources as ^{88}Y, ^{60}Co ^{137}Cs, ^{22}Na, and ^{241}Am, that cover the energy interval from 60 to 1900 keV. In these measurements, the BaF_2 detector and its associated electronics have been removed. The positions of the photoelectric peaks in the ADC spectra for this and the other explored sources show a very linear behaviour. The non-linearity coefficient [14], defined as

$$\sigma_{\mathrm{nl}} = \sqrt{\frac{1}{N}\sum_{i=1}^{N}\left(\frac{Q(E_i)}{Q(^{137}\mathrm{Cs})} - \frac{E_i}{661.6}\right)} \tag{5}$$

and summed over the seven investigated energies resulted to be: σ_{nl} (YAP) = 0.0125, σ_{nl} (LYSO) = 0.054. These values are very low compared to those in Ref. [14] that however refer to lower and different energies.

In Fig. 3 we plot Q, the charge photopeak ADC channel number, as obtained from the left ADC spectrum in coincidence with the BaF_2 detector, scanning polished YAP and LYSO crystals in the z-range from 1 to 9 cm, in steps of 1 cm. The linear behaviour in log scale means that

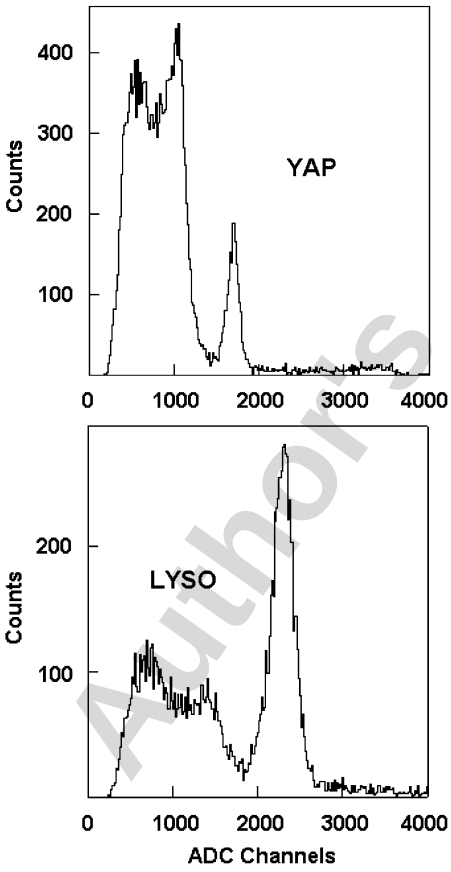

Fig. 2. Energy spectra for polished 10 cm long YAP (upper panel) and LYSO (lower panel) scintillator bars exposed to 511 keV γ-rays impinging at the centre of the crystal lateral surface. The spectra have been obtained by summing the crystal left and right ADC signals and in coincidence with the BaF_2 signal.

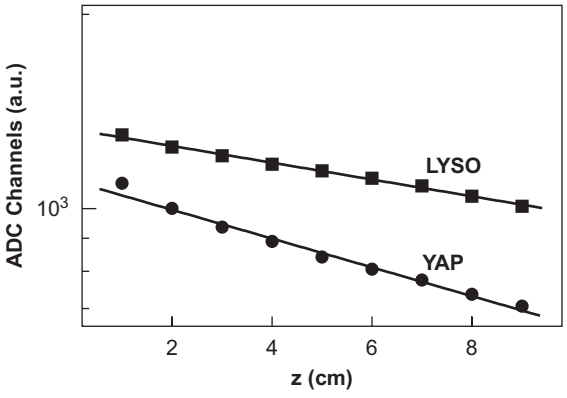

Fig. 3. The 511 keV γ-ray photopeak signal amplitude (log scale) measured at one end of the bar (here left) versus the z-position of the ^{22}Na source on the lateral surface of a polished YAP and LYSO crystal. The different slope of the two sets of points is due to the different λ_{eff} value for the two scintillators.

one exponential ($Q_0 \exp[-z/\lambda_{\text{eff}}]$) is sufficient to reproduce the PMTs pulse heights measured by changing the relative position of crystal and γ-source.

The average effective attenuation length evaluated on a set of sixteen polished YAP crystals results to be $\lambda_{\text{eff}} = 20.8 \pm 0.4$ cm. This value is higher than those reported in Refs. [2,13] and, as we will discuss below, would lead to a worse resolution of our z-reconstruction method. For a set of three polished LYSO crystals an even higher value, $\lambda_{\text{eff}} = 42.0 \pm 0.9$ cm, has been obtained. Also this value is higher than those (2–4 cm) that can be deduced from the data in [5–8,15] that however refer to LSO scintillators not mechanically polished.

In Fig. 4 we report the results of the same z-scans for YAP crystal bars with the lateral surfaces coated or wrapped. The experimental data show that also the behaviour of coated or wrapped crystals is well reproduced by one exponential. The resulting light attenuation lengths λ_{eff} are reported in Table 1. The investigated wrappings/coatings result in λ_{eff} values in the range 3.9–11.9 cm, compared to 20.8 cm for the polished uncoated YAP crystal. Although each of the wrappings/coatings can effectively reduce λ_{eff}, only the Teflon wrapping is able to practically halve it and to maintain, at the same time, a high light yield (N_0). The metallic evaporation method, on the other hand, has the advantage to allow tuning λ_{eff} to a desired value by changing the coating thickness, but it decreases the N_0 value.

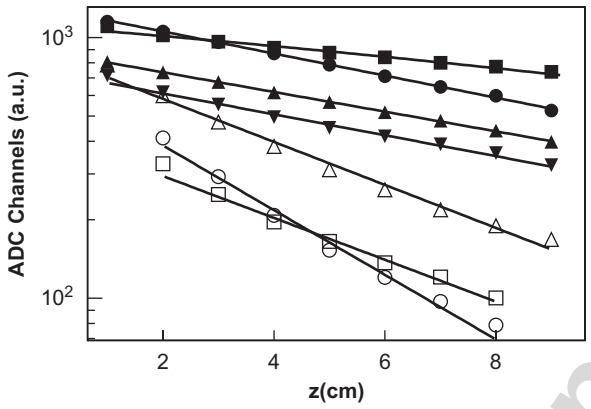

Fig. 4. Pulse height of the photopeak centroids as delivered by a H3164-10 Photomultiplier for 511 keV γ-rays impinging laterally on a 10 cm long YAP crystal at different z-positions. Full squares refer to a polished crystal, full points to a Teflon wrapped crystal, upward full triangles to a crystal coated with 1 nm Cr, downward full triangles to a white painted crystal, upward empty triangles to a crystal coated with 1.5 nm Au, empty squares to a black painted crystal, empty circles to a crystal coated with 3 nm Cr. The lines on the experimental points are exponential fits to the data, giving the light attenuation lengths λ_{eff} reported in Table 1. The extrapolation of the fits to $z = 0$ gives a rough estimate of $N_0/2$ (see Eq. (1)). The N_0 parameter is obviously also affected by the surface properties of the crystal.

The effectiveness of Teflon in reducing the photon attenuation length has also been proved for LYSO crystals. The effects of other wrappings/coatings have not been tested on LYSO because currently only few crystal samples are available. Presumably the effects are the same as for YAP.

We remark that the extrapolations of the data in Fig. 4 to $z = 0$ (which correspond to $N_0/2$) show that the light collection efficiency is strongly dependent on the wrapping/coating.

Moreover we note that the use of the exponential law (Eq. (2)) in determining the DoI (Eq. (1)) in our PET is more precise than the linear approximation ($z = L_c \times N_1/[N_1 + N_2]$) used in Refs. [5–8], based on the condition: $N_1(z) + N_2(z) = \text{const}$, not met by the data presented in Figs. 3 and 4.

The reconstructed z-coordinate of the gamma scintillation point in the crystal is derived from the ratio of signals at the left and right bar ends using Eq. (1). The mean values of the reconstructed z-coordinate for photopeak events, plotted as a function of the true z-coordinate, show a very linear behaviour. A small non-linearity has been observed at the crystal ends for the shorter λ_{eff} values.

The distributions of the reconstructed z-points for individual 511 keV gammas have a Gaussian shape whose standard deviations, giving the σ_z resolution in the z-reconstruction, are shown in Fig. 5, both for YAP (upper panel) and LYSO (lower panel) crystals, in polished (full squares) and Teflon wrapped (full circles) samples. Values of $\sigma_z = 0.8$ and 1.45 cm are found for polished YAP and LYSO, respectively, essentially constant along the crystal

Table 1
Deduced λ_{eff} and N_0 values and experimental spatial, energy and time resolutions for 10 cm long YAP and LYSO crystals polished (and surrounded by air) or covered with different coatings, obtained for scintillations of 511 keV γ-rays in the centre of the crystal

	λ_{eff} (cm)	σ_E/E (%)	σ_z (mm)	σ_t (ps)	N_0
YAP Polished	20.8±0.4	4.6±0.4	8.2±0.3	440±15	927
YAP Cr (1 nm)	11.9±0.3	5.2±0.3	7.1±0.4	480±15	850
YAP White Painted	10.7±0.2	6.2±0.3	6.5±0.2	550±20	612
YAP Tefl. wrap.	10.5±0.3	4.7±0.2	5.4±0.3	470±20	1120
YAP Black Painted	5.4±0.2	10.6±0.7	6.1±0.3	775±30	320
YAP Au (1.5 nm)	5.2±0.2	7.7±0.8	4.8±0.4	640±35	638
YAP Cr (3 nm)	3.9±0.2	13.4±1.5	5.3±0.2	925±30	284
LYSO Polished	42.0±0.9	6.2±0.2	14.4±0.4	420±10	1173
LYSO Tefl. wrap.	20.0±0.5	7.0±0.2	9.3±0.3	490±10	749

All the resolutions have been evaluated from the standard deviation of the photopeak of the sum spectra $N_1 + N_2$.

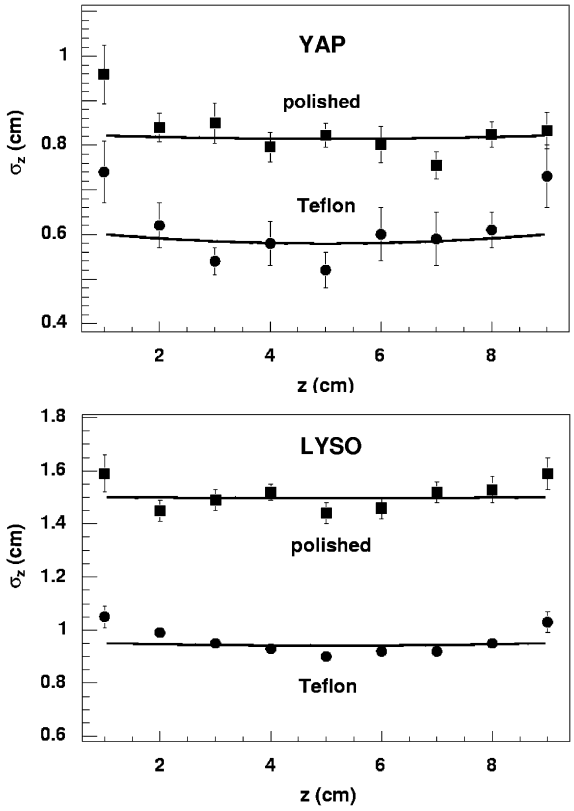

Fig. 5. The uncertainties in detecting a reconstructed scintillation point (standard deviations of the z-reconstructed distributions) versus the effective source z-position for YAP (upper panel) and LYSO (lower panel), polished (full squares) and Teflon wrapped (full circles) crystals.

length for polished crystals. The two plots show a significantly improved spatial resolution when the crystals are wrapped with Teflon tape: $\sigma_z = 0.6$ for YAP and 0.95 cm for LYSO. However the resolution slightly degrades towards the ends of the crystals. The measured σ_z values in the crystal centre ($z = 5$ cm) are reported in Table 1.

Smaller σ_z values have been reported in Refs. [5–8] for shorter LSO crystals. The best resolutions (Δz [FWHM] = 3–4 mm [5,6]) have been obtained for 2 cm long unpolished crystals, with the lateral surfaces left "as cut by the saw". A worse resolution (Δz [FWHM] = 10 mm) was obtained in Ref. [6] for a polished Teflon-wrapped 2 cm long LSO crystal.

To achieve an optimum performance both for energy and z-reconstruction resolution, the crystal has to provide a high light yield (N_0) and an adequate short effective absorption length (λ_{eff}). These two requirements are to a certain extent contradictory and therefore a good compromise is mandatory. The energy resolution σ_E/E has been derived from the standard deviation of the photopeak of the sum spectra $Q_R + Q_L$, with a ^{22}Na source positioned at the centre of the crystal ($z = 5$ cm). The data in the upper panel of Fig. 6 show the energy resolution of YAP and LYSO crystals, respectively, as a function of the λ_{eff} values obtained with the different coatings/wrappings. As expected, the energy resolution degrades with decreasing λ_{eff}, while the z-resolution, measured at $z = 5$ cm (see the central panel of Fig. 6), shows the opposite behaviour: it improves with decreasing λ_{eff}. The left–right PMT time resolution, measured at $z = 5$ cm, is displayed in the lower panel. Its behaviour is similar to that of the energy

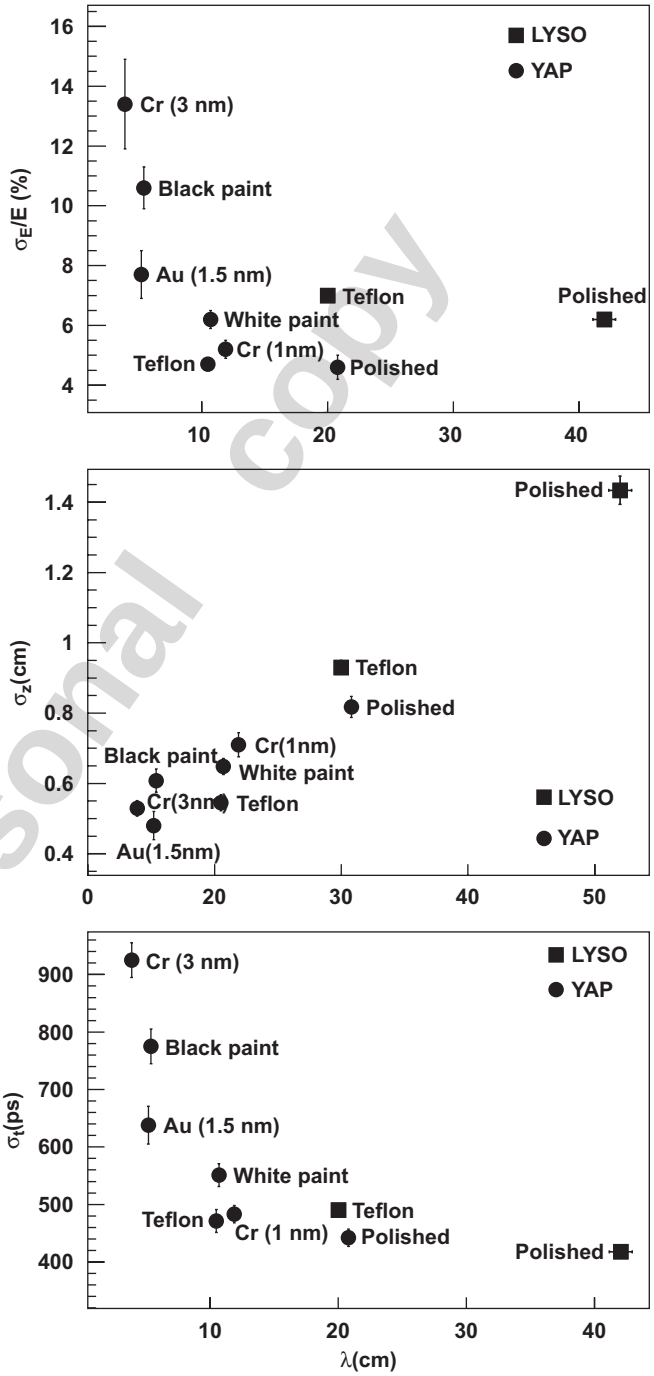

Fig. 6. The σ_E/E energy resolutions (top panel), the σ_z position resolutions (central panel), and the σ_t time resolutions (bottom panel) measured for scintillation of 511 keV γ-rays in the crystal centre ($z = 5$ cm) for YAP (full circles) and LYSO (full squares) crystals at different λ_{eff} values. All the resolutions have been evaluated from the standard deviation of the photopeak of the left and right sum spectra.

resolution. The interpretation of these data indicates that the Teflon wrapping represents a good compromise for 10 cm long YAP crystals. The experimental resolutions are summarized in Table 1 together with the N_0 values derived by assuming [2,13] an intrinsic energy resolution $(\sigma_E/E)_{intr.}$ of 1.4% and 5% for YAP and LYSO, respectively, at 511 keV, and a PMT excess noise factor value [10] of ENF = 1.4:

$$N_{pe}\left(\frac{L_c}{2}\right) = \frac{ENF}{(\sigma_E/E)^2 - R^2_{intr.}} \quad (6)$$

$$N_0 = N_{pe}\left(\tfrac{L_c}{2}\right)e^{L_{c/2\lambda_{eff}}}. \quad (7)$$

3. Conclusions

This paper is a first report on the various techniques we are exploring for the HPD-PET concept. It deals with the characterization of 10 cm long polished YAP and LYSO scintillators with 511 keV γ-rays.

Scans along the crystal bars revealed a fairly good exponential behaviour of the signal with the z-coordinate. This behaviour is observed also after wrapping or coating the crystal lateral surfaces. This allows to reconstruct the z-coordinate from the ratio of the signals measured at the two bar ends. This last result validates an important aspect of the 3D Axial PET concept.

The examined polished YAP and LYSO crystals were found to be significantly more transparent than those studied in earlier works [2,5–7,13]. The polished LYSO crystals showed a very large effective optical absorption length of about 40 cm, i.e. a bulk value of about 50 cm. The polished YAP crystals showed a shorter, but still large, effective absorption length of about 21 cm, i.e. a bulk value of about 25 cm. Wrapping or coating the crystal lateral surfaces allows decreasing the λ_{eff} value, but also influences N_0. The two parameters affect σ_z, σ_E/E and σ_t. The Teflon wrapping was found to be the best method to reduce λ_{eff} and σ_z while maintaining an acceptable N_0 value and hence also good σ_E/E and σ_t resolutions. The Cr coating allows to tune λ_{eff} to the desired value, but it decreases N_0, and thus is less effective in improving σ_z.

With a Teflon wrapping σ_E/E values of 4.7% and 7% have been obtained for YAP and LYSO crystals, respectively. The same wrapping gives σ_z values of 5.4 and 9.3 mm for YAP and LYSO crystals, respectively. The worse LYSO values are most probably caused by a higher intrinsic (non-statistical) energy resolution of this scintillator.

Both the YAP and LYSO z-resolutions are higher than values obtained in other PET design studies [5,6,8] with a read out at both crystal ends performed with raw and shorter LSO scintillators. We plan to build the 3D axial PET concept with custom designed HPDs, equipped with a thin sapphire entrance window, which leads to matched refractive indices. For Teflon wrapped YAP crystals, an improvement of 29% in the σ_z values and of 40% in the σ_E/E ones are predicted from the Litrani code [11], which follow from a 50% increase of N_0, a 13% decrease of the λ_{eff} value, and the HPD ENF value very near to 1.

Even if the best resolutions ($\Delta E/E$ (FWHM) = 8%, Δz (FWHM) = 9.8 mm) are predicted for Teflon wrapped YAP crystals, the choice of the scintillator to be used in the final project has not yet been made. Simulation calculations [11] and other experimental tests will be performed to extrapolate the presented results to other crystal lengths and to other scintillators.

References

[1] The CIMA collaboration: ⟨http://www.cima-collaboration.org/⟩.
[2] J. Seguinot et al., CERN preprint PH-EP/2004-050, Nuovo Cimento (submitted for publication).
[3] C. Joram, Nucl. Phys. B (Proc. Supp.) 78 (1999) 407.
[4] A. Braem, et al., Nucl. Instr. & Meth. A 525 (2004) 268.
[5] Y. Shao, et al., IEEE Trans. Nucl. Sci. NS49 (2002) 649.
[6] P.A. Dokhale, et al., Phys. Med. Biol. 49 (2004) 4293.
[7] J.S. Huber, et al., IEEE Trans. Nucl. Sci. NS48 (2001) 684; G.C. Wang, et al., Trans. Nucl. Sci. NS51 (2004) 775.
[8] E. Gramsch, et al., IEEE Trans. Nucl. Sci. NS50 (2003) 307.
[9] K. Shimizu, et al., IEEE Trans. Nucl. Sci. NS35 (1988) 717.
[10] C. D'Ambrosio, H. Leutz, Nucl. Instr. & Meth. A 501 (2003) 463.
[11] F.X. Gentit, ⟨http://gentit.home.cern.ch/gentit/⟩.
[12] ⟨http://www.2spi.com/catalog/ltmic/cargille-standard.shtml⟩; ⟨http://www.2spi.com/catalog/ltmic/cargille-liquid.html⟩.
[13] A. Del Guerra, et al., IEEE Trans. Nucl. Sci. NS44 (1997) 2415.
[14] P. Dorenbos, Nucl. Instr. & Meth. A 486 (2002) 208.
[15] W.W. Moses, S.E. Derenzo, IEEE Trans. Nucl. Sci. NS41 (1994) 1441; W.W. Moses, Nucl. Instr. & Meth. A 471 (2001) 209.